Article

Design, Synthesis and In Vitro Studies of 3-Amidocoumarins as Novel Antibiofilm Agents

Rajesh Kumar Sharma [1], Vineeta Singh [2], Vaishali Raghuvanshi [1] and Diksha Katiyar [1,*]

[1] Department of Chemistry, MMV, Banaras Hindu University, Varanasi 221005, India
[2] Department of Biotechnology, Institute of Engineering and Technology, Lucknow 226021, India
* Correspondence: diksha@bhu.ac.in

Abstract: *Pseudomonas aeruginosa*, a life-threatening bacteria listed as a priority pathogen by World Health Organization WHO, is known to cause severe nosocomial infections and fatality in immunocompromised individuals through its quorum sensing (QS) mediated biofilm formation. *P. aeruginosa's* antibiotic-resistant biofilms are highly challenging to the existing antibiotic treatment options. There is an urgent clinical need to develop novel alternative therapeutic molecules such as antibiofilm and antiquorum sensing agents to counter the emergence of an unprecedented pace of antibiotic resistance of pathogens. In this context, a library of seventy 3-amidocoumarin derivatives was designed, and docking studies were performed against the *P. aeruginosa* LasR receptor using AutoDock 4.0. Based on docking results, a final series of sixteen 3-amidocoumarin derivatives (**4a–p**) were synthesized and evaluated for antibiofilm activity in vitro. Eight compounds significantly inhibited the formation of *P. aeruginosa* PAO1 biofilm. Compounds **4f, 4l** and **4o** showed maximum % inhibition in antibiotic-resistant *P. aeruginosa* PAO1 biofilm formation in the range of 80% to 86%. Further, the structure–activity relationship (SAR) studies revealed that the presence of electron-donating and bromo substituents at benzamido and coumarin moieties, respectively, effectively enhances the antibiofilm activity. In addition, the binding interactions between the synthesized compounds and active sites of the LasR QS receptor (Protein Data Bank Code: 2uv0) in *P. aeruginosa* were also investigated by molecular docking. The high binding affinities indicate that these compounds might be suitable for development into potent inhibitors of QS and biofilm disruptors.

Keywords: antibiofilm activity; coumarins; inhibitors; molecular docking; *P. aeruginosa*; quorum sensing

1. Introduction

Bacterial biofilms are highly structured complex communities of bacteria held together by a self-produced extracellular polymeric matrix mainly composed of polysaccharides, secreted proteins and extracellular DNAs. Biofilms, which can be formed on biotic and abiotic surfaces, provide chemical and biological protection to the bacterium, making them physiologically distinct from planktonic cells [1]. The protective shield of biofilm gives additional resistance to the bacteria to tolerate harsh conditions and also makes them resistant to antibiotics, host–defense systems and external stresses. Current estimates show that more than 80% of bacterial infections are accompanied by biofilm formation, which contributes to pathogenesis, especially in chronic infections [2]. Biofilm can enhance the antibiotic resistance of microbial cells up to 10–1000 times more than planktonic cells [3]. Antibiotic-resistant bacterial infections not only cause huge morbidity and mortality across the world but also lead to social and economic instability for affected individuals and their families [4]. Decreased penetration of antibiotics, a decreased growth rate of the biofilm cells and/or a decreased metabolism of bacterial cells in biofilms may contribute to this tolerance [5]. Biofilm formation is a well-regulated multi-step process, and its

eradication from the site of infection by the use of present antimicrobial therapy is not often possible [6,7].

Quorum sensing (QS) plays an important role in the production of biofilms and related virulence factors, which are closely related to the regulation of bacterial resistance [8,9]. It enables bacteria to communicate with their surroundings and regulate a variety of physiological functions in a cell-density-dependent manner via the production and release of chemical signaling molecules called autoinducers. When an autoinducer attains a critical threshold, the bacteria detect and respond to this signal by altering their gene expression [10]. QS signaling systems in bacteria can be broadly classified into three main groups. Gram-positive bacteria specifically produce autoinducing peptides (AIPs) as signaling molecules, whereas Gram-negative bacteria communicate using small molecules such as the acylated homoserine lactones (AHLs). The autoinducer-2 (AI-2) signal molecule has been detected in both Gram-negative and Gram-positive bacteria [11,12].

Over recent years, several natural and synthetic molecules have been reported in the literature that can cause disruption of the QS signaling cascade by mimicking signaling molecules, thereby inactivating the QS system by blocking the receptor and preventing gene expression and biofilm formation [13,14]. Brominated furanone firstly isolated from *Delisea pulchra* (marine algae) in 1993 showed potent QS inhibitory activity [15]. Since then, several halogenated lactones and non-lactone mimics have been reported to disrupt QS signaling and biofilm formation [16,17]. In 2019, Almohaywi et al. reported dihydropyrrolones as bacterial quorum sensing inhibitors (QSIs) [18]. The most active compound of this series exhibited 63.1% QS inhibition at 31.25 μM and 60% biofilm inhibition at 250 μM. Liu et al. recently reported the biofilm inhibitory activity of some aryl-substituted pyrrolidone derivatives with IC_{50} values in the range of 0.219 to 0.281 mM against *Pseudomonas aeruginosa* PAO1 [19]. Some other non-AHL-based QSIs, such as *N*-aryl glyoxamide-based small molecules, reduced biofilm formation in *P. aeruginosa* MH602 up to 71.2% at 250 μM [20], some hydrazine-carboxamide hybrids have shown good antibiofilm activity against *P. aeruginosa* PAO1 at 100 μg/mL [21], and some marine alkaloids have also been reported as inhibitors of biofilm formation [22,23]. El-Messery et al. described the antibiofilm activity of some amide chalcones, with IC_{50} values ranging from 2.4 to 8.6 μg/mL [24]. Certain cadiolide analogs also inhibited biofilm formation in *Staphylococcus aureus* and *Enterococcus faecalis* at low concentrations [25]. In a recent contribution, trifluoromethyl substituted salicylanilide derivative has been reported to reduce preformed biofilm in *S. aureus* better than vancomycin [26].

A number of molecules belonging to the coumarin family have also been documented as antibiofilm and anti-QS agents (Figure 1) [27,28]. Some simple coumarin derivatives such as 6,7-dihydroxy, 7-hydroxy, 6-hydroxy and 3-hydroxycoumarin have been reported to cause 63, 61, 46 and 38% inhibition, respectively, of *P. aeruginosa* ATCC 27,853 biofilm formation at 100 μg/mL [29]. An important coumarin derivative warfarin, which is widely used as an anticoagulant, inhibited the biofilm formation in *Escherichia coli* by 50% at a concentration of 5 mM in the presence of lactoferrin and ampicillin [30]. These two compounds have been reported to promote biofilm formation in *E. coli* when administered at subinhibitory concentrations. A recent study described the inhibitory action of the coumarin scaffold on *P. aeruginosa* PAO1 biofilm formation in a dose-dependent manner; biofilm formation was inhibited by 9.98, 21.51, 33.16 and 46.10% at 31.25, 62.5, 125 and 250 μg/mL, respectively, with respect to the control [31]. Though a number of natural and synthetic compounds have been reported as inhibitors of QS and biofilm formation, so far, none of these have reached the clinics. Therefore, there is an urgent requirement for new antibiofilm agents. Here, we report the design and synthesis of 3-amidocoumarin as *P. aeruginosa* PAO1 biofilm inhibitors.
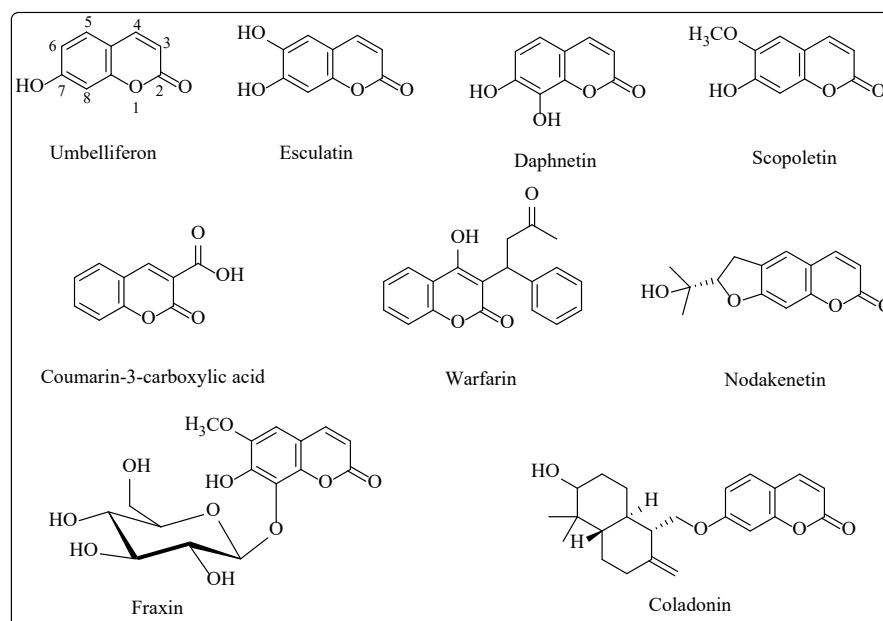
Figure 1. Chemical structures of coumarin compounds possessing anti-QS and antibiofilm activity.

Inhibitor Design

Recent reports on the role of coumarins in the disruption of biofilm formation and QS signaling without disturbing planktonic cell growth have drawn the attention of many researchers to develop these molecules as novel antibiofilm agents. Studies also have revealed that substitutions at specific sites resulted in enhancement of activity while at other positions led to diminishing activity [27–29]. Thus, suitably substituted coumarins provide a good choice for the development of antibiofilm agents. In our earlier investigations, we reported the antibacterial activity of a series of twenty-three amidocoumarins [32]. These compounds comprised coumarin heterocycle containing lactone ring and a substituted amido group at position 3, and both these moieties are also present in a number of antibiofilm agents and QSIs [Figure 2: color coding depicts different components: coumarin moiety (yellow), amide group (red ellipse), bromine (green) and lactone (blue rectangle)]. Therefore, we envisaged to evaluate the QS inhibitory activities of these amidocoumarins as a mechanistic approach for biofilm inhibition using *Chromobacterium violaceum* CV026 as a reporter strain by a method reported by Shukla et al. [33]. *C. violaceum* is a Gram-negative bacterium, which utilizes AHLs as signaling molecules for QS. Hence, this strain is widely used in research work related to QSI screening [25]. Out of twenty-three amidocoumarins tested, six compounds S1–S6 (Figure S1) showed anti-QS activity with zones of inhibition 14, 15, 14, 12, 16 and 14 mm, respectively, against *C. violaceum*. The remaining compounds of the series showed low/minimal activity, which suggested that compounds S1-S6 might have a specific biofilm formation inhibitory potential than the rest of the compounds. Therefore, we considered further substitutions/modifications of compounds S1–S6 to develop them as potent antibiofilm agents. Initially, a library of forty-eight compounds with appreciable diversity was designed by introducing 6,8-dicloro (a), 6-bromo (b), 6-chloro (c), 6-nitro (d), 8-methoxy (e), 6-methyl (f), 7-hydroxy (g) and 8-methoxy substituent (h) on the coumarin ring of S1–S6 precursor molecules, to obtain six sets, each containing eight molecules S1a–h to S6a–h (Supporting Information Tables S1–S6). All these compounds showed a good binding affinity with the active site of *P. aeruginosa* LasR (PDB Code: 2uvo) receptor with binding energies in the range of −8.25 to −11.95 kcal/mol. Among them, the binding energies of compounds with the 6-bromo substituent (S1b–S3b, S5b, S6b) were the best in each set with the exception of S4b. In previously reported work, bromine substituent has also delivered promising results for QS and biofilm inhibition [16,18]. We further designed twelve more compounds by introducing the bromo group on the C-5 and C-7 positions of

the coumarin ring (Supporting Information Table S7, compounds S1i,j to S6i,j) of precursor molecules S1–S6, but most of these compounds exhibited low binding affinity (i.e., higher binding energy values) with the receptor as compared to their C-6 bromo analogs. Further, to obtain better SAR, we constructed five new coumarin derivatives S7–S11 by introducing different amido substituents at the C-3 position of the coumarin ring and also designed their 6-bromo derivatives S7a to S11a (Supporting Information Table S8). These compounds also exhibited good binding affinity with the LasR receptor. Finally, based on the docking results and synthetic accessibility, a series of sixteen 3-amidocoumarins containing five newly designed compounds with unsubstituted coumarin ring (S7–S11) and eleven bearing the 6-bromo substituent (S7a–11a and S1b–S6b) were synthesized for testing antibiofilm activity. Hereafter, the synthesized 3-amidocoumarins have been re-designated as **4a–4p** and their detailed synthesis procedure, molecular docking and bioactivity results are described here. The docking poses of **4a-4p** in complex with *P. aeruginosa* Las R receptor are shown in Figure S2.
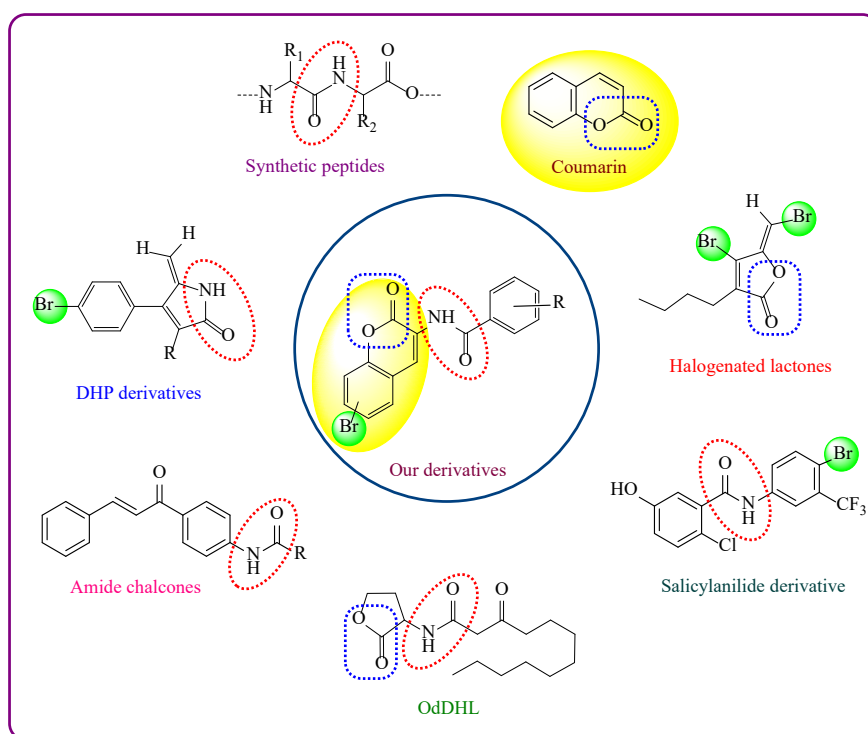

Figure 2. Rational design of our synthesized compounds.
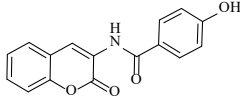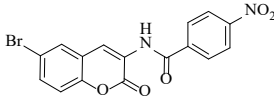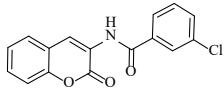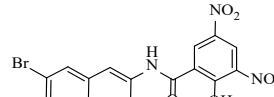
2. Results and Discussion
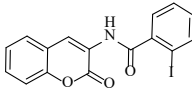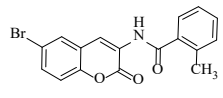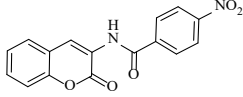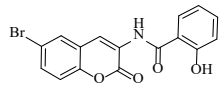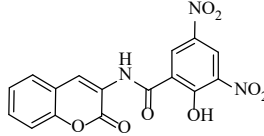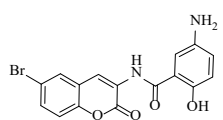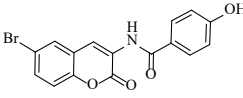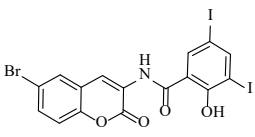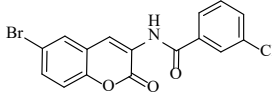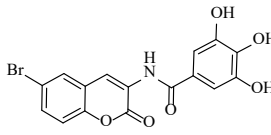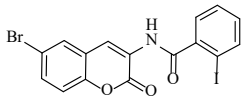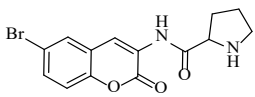
2.1. Chemistry

The synthetic route for the preparation of coumarin compounds is depicted in Scheme 1. 3-Nitrocoumarin **1a** and 6-bromo-3-nitrocoumarin **1b** were prepared via L-proline catalyzed condensation of ethyl nitroacetate and salicylaldehyde as reported earlier [34]. Nitrocoumarins **1a** and **1b** were reduced to 3-aminocoumarin **2a** and 3-amino-6-bromocoumarin **2b**, respectively, using acidified $SnCl_2$. 3-Amidocoumarins **4a–p** were prepared by reaction of **2a** and **2b** with suitable carboxylic acids **3a–p** using PCl_3 in acetonitrile under reflux for 5 to 6 h by slight modification in earlier reported method [32]. The structures of all the synthesized compounds were established on the basis of IR, ^1H and ^{13}C NMR and mass spectral data. Spectral data of compound **4a** are shown in Figures S3–S6. The log *P* values were calculated using the ChemDraw 16.0 program (Table 1).
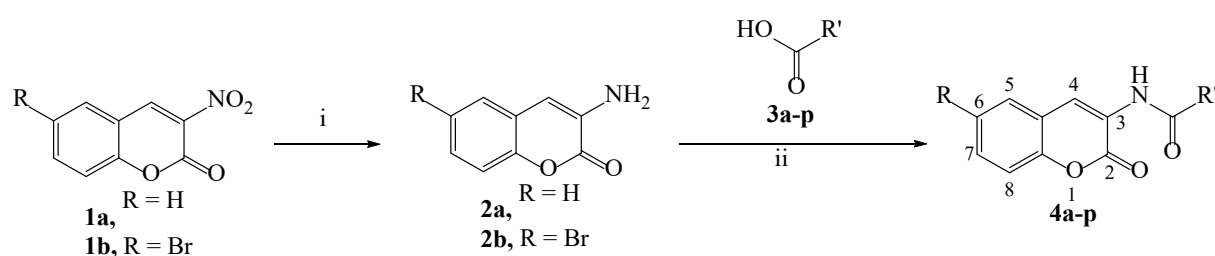
Scheme 1. Synthesis of 3-amidocoumarins. (i) SnCl$_2$, HCl, rt (ii) PCl$_3$, CH$_3$CN, reflux.

Table 1. Synthesized amidocoumarin derivatives **4a–4p** and their log *P* and binding energy (kcal/mol) values.

Synthesized Compounds		log *P*	Binding Energy	Compound		log *P*	Binding Energy
4a		1.72	−11.36	**4i**		3.62	−10.52
4b		2.67	−10.51	**4j**		3.20	−10.31
4c		3.47	−10.32	**4k**		3.43	−11.25
4d		2.74	−9.84	**4l**		2.55	−11.66
4e		2.31	−10.46	**4m**		1.75	−11.31
4f		2.55	−11.47	**4n**		5.26	−9.44
4g		3.50	−10.68	**4o**		1.77	−11.69
4h		4.30	−11.65	**4p**		0.95	−11.03

2.2. Biology

Initial screening of the coumarin compounds was performed with antimicrobial testing by the minimum inhibitory concentration (MIC) method. Results were not promising, and the compounds showed very poor antibacterial activity against the tested bacterial strains *C. violaceum* and *P. aeruginosa*. This inactivity further suggested that the compounds have no ability to interfere with the primary bacterial metabolism and have little effect on bacterial growth [19]. The compounds were next examined for biofilm inhibition activity against *P. aeruginosa* PAO1. Hentzer et al. reported that the genes responsible for the quorum sensing are present in the strain *P. aeruginosa* PAO1, which was considered in the present

study [35]. Hence, the biofilm inhibitory activity of the synthesized compounds against *P. aeruginosa* may be due to the quorum quenching activity. An ideal QS inhibitor should possess high QS inhibition to minimize the production of bacterial virulence factors and biofilms while having minimal bacterial growth inhibition to reduce the likelihood of bacteria developing drug resistance.

The biofilm inhibition test was performed against the *P. aeruginosa* PAO1 bacterial strain using a crystal violet stain [33]. The assay results revealed significant biofilm inhibition by some of the compounds at 100 µg/mL. **4l**, followed by **4o, 4f, 4a** and **4h** with 86%, 82%, 80%, 76% and 72% inhibition, respectively, were the most potent antagonists of biofilm formation (Figure 3). Importantly, **4f, 4g, 4h**, and **4i** with the 6-bromo-substituted coumarin ring displayed superior biofilm inhibition activity compared to their precursors **4a, 4b, 4c** and **4d** with the exception of **4j**, which showed 50% inhibition in comparison to **4e** (68%). These results suggest that bromo substitution is tolerated and enhances biofilm inhibitory activity. **4c, 4d, 4i, 4k, 4m** and **4p** showed biofilm inhibitory properties in the range of 50–72%, while **4n** (log *P* = 5.26) with 30% inhibition was not effective in biofilm dispersal, which may be due to reduced cell permeability or steric hindrance caused by bulkier halogen atoms.
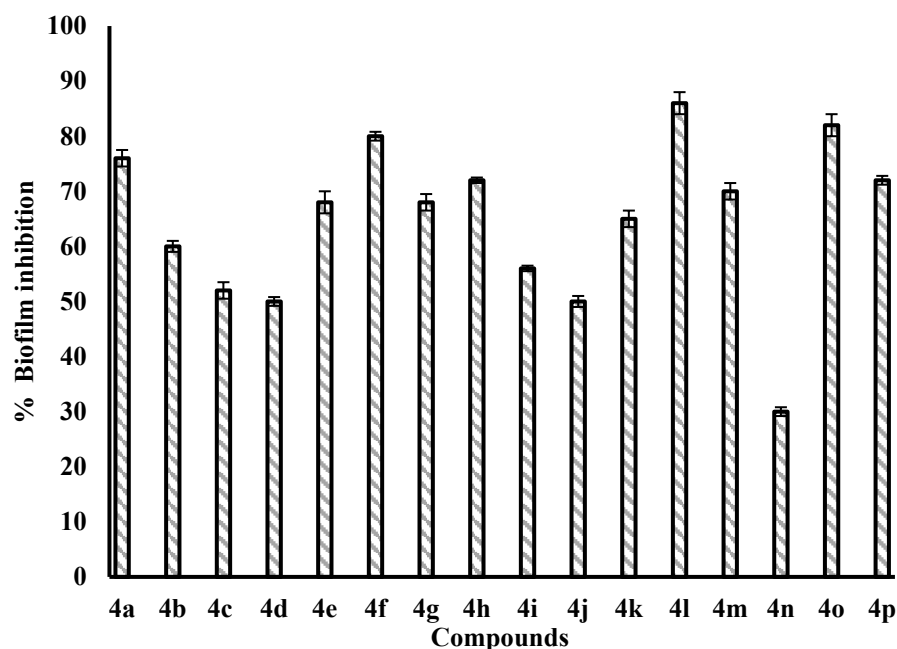
Figure 3. Biofilm inhibition in *P. aeruginosa* PAO1 by the synthesized compounds under experimental conditions of 100 µg/mL concentration.

The nature of substituents present on the amido phenyl ring significantly influenced the biofilm activity. Compounds containing hydroxyl and amino groups (**4a, 4f, 4l, 4m** and **4o**) showed greater biofilm inhibition, whereas substitution of chloro and nitro groups (**4b, 4d, 4g, 4i** and **4j**) led to a decrease in biofilm inhibition. Compounds **4k** and **4p** with Ar-CH$_3$ and proline groups displayed moderate activity with 65% and 72% inhibition. **4l** bearing o-OH at the phenyl ring and bromo group at the C-6 position of the coumarin nucleus displayed the highest antibiofilm activity (86%) amongst all the synthesized coumarins. Overall, the synthesized compounds exhibited moderate to excellent levels of biofilm inhibition against *P. aeruginosa*. Some compounds were found to be superior in inhibiting the formation of biofilm than recently reported antibiofilm agents. At 100 µg/mL, seven compounds of the series exhibited more than 70% inhibition. These compounds also exhibited good affinity with the binding pocket of LasR protein with binding energy values less than −11 kcal/mole, which suggests that the biofilm inhibitory activity of these amidocoumarins might be due to the disruption in QS signaling.

2.3. Docking Studies

To identify binding orientations, all the compounds were docked into the crystal structure of *P. aeruginosa* LasR (PDB Code: 2uv0) with the autoinducer *N*-3-(oxododecanoyl)-L-homoserine lactone (*OdDHL*) [36] using the AutoDock 4.0 (The Scripps Research Institute, La Jolla, CA, USA) program. Compounds interacted with the amino acid residues of the active pocket, consisting of 17 amino acid residues including Leu36, Gly38, Leu39, Tyr64, Leu125, Gly126, Ala127, Trp60, Asp73, Tyr56, Ser129, Thr75, Ala105, Trp88, Leu110, Tyr93 and Arg61, with binding energy values ranging from −9.44 to −11.69 kcal/mol. The docking results of the top seven compounds are presented in Table 2. The docking results were mainly interpreted on the basis of (i) orientation of docked compounds relative to natural ligand OdDHL, (ii) intermolecular interactions present between the compound and target and (iii) binding energies of the docked compounds with the reference OdDHL.

Table 2. Docking of compounds into the LasR receptor protein of *P. aeruginosa*.

Entry	Binding Energy (kcal/mol)	Pose No.	Orientation *	H-Bond Interaction	Electrostatic Interaction	Hydrophobic and π Interactions
OdDHL (crystal str)	-		-	Trp60, Asp73, Tyr56, Ser129	Tyr56, Tyr64, Asp73, Thr75, Ala105, Ser129	Tyr47, Tyr64, Tyr93, Ala105, Leu110, Gly126
OdDHL (Docked)	−9.48	1	Similar	Tyr56, Ser129, Tyr93, Thr75	Trp88, Ala105, Phe101, Asp73, Leu110	Leu36, Gly38, Leu39, Leu40, Tyr64, Leu125, Gly126, Ala127
4o	−11.69	7	Flipped	Val111, Tyr93, Ser129, Tyr56, Arg61	Leu36, Gly38, Trp88, Tyr64, Leu110, Asp73, Thr75, Ala105, Gly126, Ala127	Leu36, Gly38, Ala127, Val76, Trp88, Tyr64
4l	−11.66	7	Flipped	Ser129, Trp60, Arg61	Leu36, Gly38, Tyr64, Tyr56, Asp73, Leu110, Gly126, Ala127	Leu36, Gly38, Ile52, Tyr64, Thr75, Trp88, Tyr93, Ala105, Leu110
4h	−11.65	9	Similar	Trp60, Arg61	Tyr47, Leu36, Trp60, Arg61, Tyr56, Asp73, Trp88, Tyr93, Val76, Tyr64, Thr75	Leu36, Leu39, Gly38, Ala50, Tyr56, Trp60, Tyr64, Gly126, Ala127
4f	−11.47	4	Flipped	Leu110, Tyr93, Ser129, Tyr56, Arg61	Leu36, Gly38, Leu39, Trp88, Tyr64, Asp73, Leu110, Leu125, Gly126, Ala127	Leu36, Gly38, Ile52, Tyr64, Thr75, Trp88, Leu110
4a	−11.36	8	Flipped	Tyr56, Arg6, Tyr93, Val111, Ser129	Leu36, Tyr64, Trp88, Leu110, Asp73	Leu36, Gly38, Trp88, Thr75, Ala127
4m	−11.31	7	Flipped	Tyr93, Ser129, Trp60, Arg61	Leu36, Gly38, Trp88, Tyr56, Tyr64, Asp73, Thr75, Leu110, Gly126, Ala127	Leu36, Gly38, Tyr64, Trp88, Ala105, Leu110
4k	−11.25	10	Flipped	Tyr56, Arg61, Ser129	Leu36, Gly38, Leu39, Tyr64, Asp73, Leu125, Gly126, Ala127	Leu36, Gly38, Ile52, Trp60, Tyr64, Thr75, Trp88, Tyr93, Leu110

* In respect of orientation of OdDHL (crystal str).

The crystal structure of the *P. aeruginosa* LasR ligand-binding domain (LasR-LBD) bound to its autoinducer OdDHL reveals that the polar region, including the lactone ring and carbonyl groups, of OdDHL form six intermolecular H-bonds with LasR-LBD. Five direct H-bonds are formed between (i) the lactone carbonyl and NH of Trp60 (3.01 Å), (ii) the amide NH and the carboxyl group of Asp73 (2.76 Å) and Thr75 (3.39 Å), and (iii) amide 1-oxo with the hydroxyl groups of Ser129 (2.70 Å) and Tyr56 (2.65 Å). An

indirect H-bond is formed between the 3-oxo group and a water molecule and then with Arg61. The long 12-carbon acyl chain buries into the cavity lined with several hydrophobic residues [36].

We also manually positioned the autoinducer *OdDHL* into the receptor binding site for a better understanding of the binding interactions (Table 2). The docking analysis suggests that the lactone ring of OdDHL interacts with the lactone pocket and forms four H-bonds between (i) carbonyl lactone and Trp-60 (2.80Å), (ii) NH of amide and Asp-73 side chain (2.19Å), (iii) amide carbonyl and Ser129 side chain (2.73 Å), and (iv) acyl carbonyl and Try64 (3.01 Å). The 12-carbon acyl chain inserts into the hydrophobic pocket and adopts a similar conformation to that of the LasR-OdDHL crystal complex.

Amongst all the docked compounds, **4o** having a binding energy of −11.69 kcal/mol showed the maximum binding affinity with the receptor (Figure 4). **4o** contains three hydroxyl groups and forms seven H-bonds with the LasR receptor. The lactone carbonyl formed an H-bond with Arg61 (3.33 Å), and amide carbonyl formed two H-bonds, one with Ser129 (2.80 Å) and the second with Tyr56. The hydroxyl groups formed four H-bonds with Tyr93 (2.68, 2.10, and 2.89 Å) and Leu110 (2.22 Å) side chains. The trihydroxyphenyl ring was stabilized by π–π interaction with Trp88 and Tyr56 and electrostatic interactions with Trp88, Tyr93, Ala105, Leu110 and Thr75. Bromine interacted with Gly38, Gly126 and Ala127 through hydrophobic interactions. The molecule was stabilized by hydrophobic and electrostatic interaction by Val76, Leu36, Tyr64 and Asp73 amino acid residues.
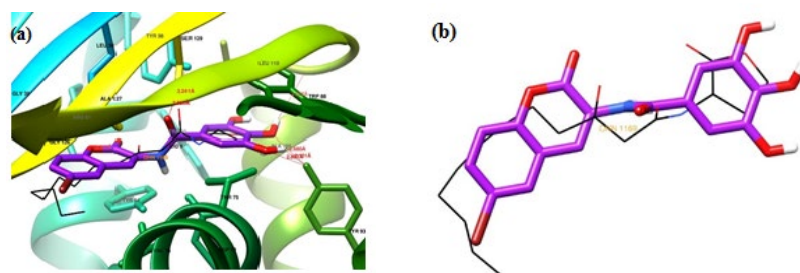

Figure 4. (**a**) Binding mode of compound **4o** (violet) within the LasR binding site in comparison with OdDHL (black lines). (**b**) **4o** (violet) superimposed on the X-ray structure of OdDHL (black lines) from the LasR complex.

4l showed a binding energy value of −11.66 kcal/mol. The coumarin ring exhibited hydrophobic interaction with Ile52, Leu36, Gly38 and π–π stacking with Tyr64. The *ortho*-hydroxyphenyl ring also exhibited π–π stacking with Trp88 and hydrophobic interaction with Leu110, Tyr93 and Thr75. This compound displayed four H-bonds between (i) the carbonyl of the amido group and the hydroxyl of Ser129, (ii) the lactone carbonyl of coumarin and the terminal NH_2 of Arg61, (iii) the lactone carbonyl of coumarin and the NH of Arg61, and (iv) the hydroxyl group and NH of Trp60. **4h** with a binding energy of −11.65 kcal/mol was docked in a similar orientation as OdDHL, with the lactone ring being inserted in the lactone pocket, while the aromatic amido group occupies the hydrophobic pocket. However, the interactions were somewhat different than OdDHL. The lactone carbonyl formed two H-bonds with Arg61. The additional H-bond was formed between the lactone ring oxygen and the Trp60 side chain. The coumarin ring showed π-stacking with Tyr64 and Tyr56, whereas bromine exhibited interaction with Trp88. Aromatic rings showed hydrophobic interactions with Asp73, Thr75, Gly38, Leu39, Ala50 and Ala127. Amide carbonyl and NH and lactone carbonyl showed electrostatic interactions with Leu36. Iodine groups showed van der Waals contacts with Tyr47, Arg61 and Tyr64.

Compound **4f** with a binding energy of −11.47 kcal/mol formed five H-bonds: two between amido carbonyl and Ser129 (2.85 Å) and Tyr56 (3.30 Å); likewise, in **4o**, *p*-hydroxyl formed H-bonds with Tyr93 (2.95 Å) and Val111 (2.05 Å), and another H-bond was formed between lactone carbonyl and Arg61 (3.25 Å). The coumarin ring in **4f** showed hydrophobic interactions with Ile52 and Gly38, whereas bromine exhibited van der Waals interactions

with Gly38, Leu39, Leu125, Gly126 and Ala127. The coumarin and amide group was stabilized by electrostatic interactions with Tyr64, Leu36 and Asp73. The *para*-hydroxyphenyl ring of **4f** formed a hydrophobic interaction with Thr75, Tyr56, Leu110 and π-stacking with Trp88. Compound **4a** displayed similar H-bonding, electrostatic, hydrophobic and π–π stacking interactions like **4f**. The binding energy of **4a** was calculated as −11.36 kcal/mol. **4m** showed similar interactions as that of **4f.** The amino group of **4f** formed a hydrogen bond interaction with Tyr93. **4k** with a binding energy of −11.25 kcal/mol showed hydrophobic interactions with Tyr56, Trp60, Leu110, Thr75 and Tyr93 and π-stacking with Trp88.

The docking results of the LasR-synthesized compounds complex revealed that all the compounds docked in the 'flipped orientation' relative to OdDHL except **4h.** Possibly, the presence of large iodine groups makes compound **4h** more lipophilic and more suited to the hydrophobic ligand-binding pocket of the receptor resulting in a similar orientation as that of OdDHL. All the compounds formed H-bond between (i) lactone carbonyl and Arg61 and (ii) amide carbonyl and Ser129 except **4h.**

3. Materials and Methods

3.1. Experimental

General: Reagents and starting materials were purchased from commercial suppliers (SRL (Gurgaon, India), Alfa Aesar (Haverhill, MA, USA), Sigma-Aldrich (St. Louis, MO, USA) and Spectrochem Pvt. Ltd. (Mumbai, India)) and used without any purification unless otherwise stated. The melting points were determined in open capillary tubes on Buchi B-510 apparatus. IR spectra were recorded on a JASCO FTIR 4700 in KBr from 400 to 4000 cm^{-1}. Analytical thin-layer chromatography (TLC) was performed on 60 F$_{254}$ silica gel precoated aluminum plates with a 0.25 mm thickness. The spots were located under a UV lamp (λ$_{max}$ = 254 nm) or stained with iodine or Dragendorff's reagent solution. ^{1}H and ^{13}C NMR were recorded on a JEOL NMR spectrometer at 500 and 125 MHz, respectively. Chemical shifts for ^{1}H NMR are reported as δ values, and coupling constants are in hertz (Hz). The following abbreviations were used for spin multiplicity: singlet (s), doublet (d), triplet (t), double doublet (dd), multiplet (m), broad singlet (bs), and if the pattern of splitting could not be interpreted easily, they are assigned as multiplet (m). Synthesized compounds were isolated by column chromatography on silica gel (60–120 mesh). Mass spectra were recorded on Sciex-X500R QTOF.

3.2. Chemistry

3.2.1. Preparation of 3-nitrocoumarin **1a** and 6-bromo3-nitrocoumarin **1b**

Compounds **1a** and **1b** were prepared based on a literature method [34]. 3-Nitrocoumarin **1a** was prepared by reaction between salicylaldehyde (0.10 mL, 1 mmol) and ethyl nitroacetate (0.11 mL, 1 mmol) using L-proline (30 mol%) as catalyst in ethanol (3 mL), whereas, 6-bromo-3-nitrocoumarin **1b** was prepared by reaction between 5-bromo-3-hydroxy benzaldehyde (0.20, 1 mmol) and ethyl nitroacetate (0.11 mL, 1 mmol).

Compound **1a**: Yellow solid, yield: 85%, mp 142–143 °C (literature [34]: 141–142 °C); ^{1}H NMR (CDCl$_3$): 8.78 (s, 1H), 7.81 (d, *J* = 7.5 Hz, 1H), 7.73 (m, 1H), 7.46 (m, 2H).

Compound **1b**: Pale yellow solid, yield: 74%, mp 198–199 °C (literature [37]: 200 °C); ^{1}H NMR (CDCl$_3$): 8.86 (s, 1H), 7.92 (d, *J* = 2.7 Hz, 1H), 7.63 (dd, *J* = 9.0 and 2.7 Hz, 1H), 7.38 (d, *J* = 9.0 Hz, 1H).

3.2.2. Preparation of 3-aminocoumarin **2a** and 6-bromo-3-aminocoumarin **2b**

Compounds **2a** and **2b** were prepared by reduction of compounds **1a** and **1b**, respectively, as described in previous work [32].

Compound **2a**: Off white solid; yield: 72%, mp 137–138 °C (literature [32]: 136–138 °C); ^{1}H NMR (CDCl$_3$): 7.33 (m, 2H), 7.18 (m, 2H), 6.67 (s, 1H), 4.29 (bs, 2H).

Compound **2b**: Off white solid; yield: 68%, mp 207–208 °C (literature [38]: 208–209 °C); ^{1}H NMR (CDCl$_3$): 7.41(d, *J* = 2.5 Hz, 1 H, H-5), 7.29 (dd, *J* = 8.5 and 2.5 Hz, 1H, H-7), 7.16 (d, *J* = 8.7 Hz, 1H, H-8), 6.58 (s, 1H, H-4), 4.32 (bs, 2H, NH$_2$).

3.2.3. General Procedure for the Synthesis of Compounds (**4a–p**)

3-aminocoumarin **2a** (1 mmol) and appropriate aromatic acid **3a–e** (1.1 mmol) were stirred in 5 mL of CH$_3$CN at room temperature for half an hour. PCl$_3$ (3 mmol) was added dropwise to the reaction mixture and refluxed for 5–6 h. After completion of reaction (monitored by TLC), the reaction mixture was quenched by adding ice-cold water (5 mL), and CH$_3$CN was evaporated under reduced pressure. A 30 mL volume of water was added to the remaining aqueous layer and the product was extracted with CHCl$_3$ (2 × 40 mL). The combined organic layers were washed twice with water (2 × 20 mL) and then with saturated NaHCO$_3$ solution (20 mL) and finally with brine (20 mL). The organic layer was collected, dried over anhydrous Na$_2$SO$_4$ and evaporated under reduced pressure to afford the crude products. The crude products were recrystallized from ethanol to yield pure samples of **4a–4d**. Compound **4e** was purified by column chromatography using hexane: ethylacetate (7:3) as eluent.

3-amidocoumarins **4f–p** were prepared by reacting 6-bromo-3-aminocoumarin **2b** (1 mmol) with appropriate carboxylic acid **3f–p** using the same procedure as described above for the synthesis of compounds **4a–4e**. The crude products in the case of **4f–4i**, **4k,** **4l, 4n** and **4o** were recrystallized from ethanol. Compounds **4m, 4j** and **4p** were purified by coluumn chromatography using hexane:ethylacetate (7:3) as eluent.

4-Hydroxy-*N*-(2-oxo-2*H*-chromen-3-yl)benzamide (**4a**)

The title compound was prepared from **2a** (0.16 g, 1.0 mmol) and 4-hydroxy benzoic acid **3a** (0.15 g, 1.1 mmol) according to general procedure, to give off white solid. Yield: 48%; m.p.: 135–137 °C; Rf = 0.55 (hexane-ethyl acetate, 3:1); IR (KBr): 3445, 3078, 1710, 1606, 1515, 1426, 1273 cm^{-1}; ^{1}H NMR (DMSO-d$_6$): δ 10.84 (s, 1H, OH), 8.58 (s, 1H, H-4), 8.28 (s, 1H, ArH), 8.11 (m, 1H, ArH), 7.66 (d, J = 7.5 Hz, 1H, H-5), 7.47 (m, 1H, H-7), 7.32 (m, 4H, H-6, H-8 and 2ArH); ^{13}C NMR (DMSO-d$_6$/CDCl$_3$; 1:1): δ 164.7, 157.5, 157.3, 150.1, 149.8, 137.7, 130.0, 127.9, 127.3, 124.8, 123.4, 119.8, 119.0, 115.7. HRMS (ESI) m/z: calcd. for C$_{16}$H$_{11}$NO$_4$ [M + H]$^+$: 282.0766, found: 282.0463.

3-Chloro-*N*-(2-oxo-2*H*-chromen-3-yl)benzamide (**4b**)

The title compound was prepared from **2a** (0.16 g, 1.0 mmol) and 2-chloro benzoic acid **3b** (0.17 g, 1.1 mmol) according to general procedure, to yield a white solid. Yield: 65%; m.p.: 150–151 °C; Rf = 0.46 (hexane-ethyl acetate, 3:1); IR (KBr): 3378, 3079, 3039, 1714, 1675, 1594, 1368, 1239 cm^{-1}; ^{1}H NMR (CDCl$_3$): δ 8.91 (s, 1H, NH), 8.85 (s, 1H, H-4), 7.75 (d, J = 7.0 Hz, 1H, H-5), 7.54 (d, J = 7.0 Hz, 1H, ArH), 7.45 (m, 2H, ArH and H-7), 7.38 (m, 1H, ArH), 7.33 (m, 3H, H-6, H-8 and ArH); ^{13}C NMR (CDCl$_3$): δ 165.3, 158.7, 150.1, 133.9, 132.4, 131.1, 130.8, 130.3, 130.0, 128.0, 127.4, 125.3, 124.1, 124.0, 119.8, 116.5. HRMS (ESI) m/z: calcd. for C$_{16}$H$_{10}$ClNO$_3$ [M + H]$^+$: 299.0349, found: 299.0343.

2-Iodo-*N*-(2-oxo-2*H*-chromen-3-yl)benzamide (**4c**)

The title compound was prepared from **2a** (0.16 g, 1.0 mmol) and 2-iodo benzoic acid **3c** (0.27 g, 1.1 mmol) according to general procedure, to yield an off white solid. Yield: 88%; m.p.: 124–126 °C; Rf = 0.42 (hexane-ethyl acetate, 3:1); IR (KBr): 3342, 3062, 1693, 1682, 1582, 1466, 1403, 1267 cm^{-1}; ^{1}H NMR (DMSO-d$_6$): δ 9.11 (s, 1H, NH), 8.69 (s, 1H, H-4), 7.96 (m, 2H, ArH), 7.68 (m, 2H, H-5 and ArH), 7.46 (m, 2H, H-7 and ArH), 7.21 (m, 2H, H-6 and H-8); ^{13}C NMR (DMSO-d$_6$): δ 168.2, 158.7, 150.2, 148.0, 140.5, 137.0, 132.5, 131.3, 130.0, 128.2, 126.8, 125.1, 124.0, 119.6, 116.4, 94.0. HRMS (ESI) m/z: calcd. for C$_{16}$H$_{10}$INO$_3$ [M + H]$^+$: 391.9783, found: 391.4968.

4-Nitro-*N*-(2-oxo-2*H*-chromen-3-yl)benzamide (**4d**)

The title compound was prepared from **2a** (0.16 g, 1.0 mmol) and 4-nitro benzoic acid **3d** (0.18 g, 1.1 mmol) according to general procedure, to yield a pale yellow solid. Yield: 86%; m.p.: 166–168 °C; R_f = 0.39 (hexane-ethyl acetate, 3:1); IR (KBr): 3373, 3115, 1694, 1607, 1540, 1430, 1350, 1294 cm^{-1}; ^{1}H NMR (DMSO-d$_6$): δ 8.93 (s, 1H, NH), 8.61 (s, 1H, H-4), 8.26 (m, 2H, ArH), 8.13 (m, 2H, ArH), 7.64 (d, *J* = 8.0 Hz, 1H, H-5), 7.49 (m, 1H, H-7), 7.31 (m, 2H, H-6 and H-8); ^{13}C NMR (DMSO-d$_6$): δ 163.9, 159.6, 151.6, 148.1, 141.2, 134.6, 129.9, 128.8, 128.2, 126.8, 125.4, 125.3, 123.2, 122.6, 121.6, 116.5. HRMS (ESI) *m/z*: calcd. for C$_{16}$H$_{10}$N$_2$O$_5$ [M + H]$^+$: 311.0668, found: 311.0662.

2-Hydroxy-3,5-dinitro-*N*-(2-oxo-2*H*-chromen-3-yl)benzamide (**4e**)

The title compound was prepared from **2a** (0.16 g, 1.0 mmol) and 3,5-dinitrosalicylic acid **3e** (0.25 g, 1.1 mmol) according to general procedure, to yield a light brown solid. Yield: 72%, Rf = 0.42 (hexane-ethyl acetate, 3:2); IR (KBr): 3016, 1716, 1672, 1529, 1337, 1265 cm^{-1}; ^{1}H NMR (DMSO-d$_6$): δ 13.45 (s, 1H, OH), 8.79 (m, 2H, ArH), 8.53 (s, 1H, H-4), 7.66 (m, 1H, H-5), 7.43 (m, 1H, H-7), 7.29 (m, 2H, H-6 and H-8); ^{13}C NMR (DMSO-d$_6$): δ 169.1, 164.4, 158.1, 150.0, 141.3, 130.5, 129.8, 128.4, 128.3, 125.7, 125.5, 125,4, 123.1, 122.7, 120.4, 116.3. HRMS (ESI) m/z: calcd. for C$_{16}$H$_9$N$_3$O$_8$ [M + H]$^+$: 372.0468, found: 372.0462.

N-(6-bromo-2-oxo-2*H*-chromen-3-yl)-4-hydroxybenzamide (**4f**)

The title compound was prepared from **2b** (0.24 g, 1.0 mmol) and 4-hydroxy benzoic acid **3f** (0.15 g, 1.1 mmol) according to general procedure, to yield an off white solid. Yield: 88%; m.p.: 193–195 °C; Rf = 0.48 (hexane-ethyl acetate, 3:1); IR (KBr): 3568, 3230, 3066, 1712, 1604, 1515, 1428, 1362, 1275 cm^{-1}; 1H NMR (DMSO-d$_6$): δ 10.1 (s, 1H, OH), 8.32 (s, 1H, H-4), 7.69 (s, 1H, H-5), 7.59 (m, 2H, Ar-H), 7.41 (m, 1H, H-7), 6.88 (d, J = 9.0 Hz, 1H, H-8), 6.75 (m, 2H, ArH); ^{13}C NMR (DMSO-d$_6$): δ 168.7, 167.5, 155.9, 151.0, 134.6, 133.1, 132.4, 130.6, 129.2, 125.3, 123.2, 122.8, 118.8, 118.7, 116.2, 110.7. HRMS (ESI) m/z: calcd. for C$_{16}$H$_{10}$BrNO$_4$ [M + H]$^+$: 359.9871, found: 359.4998.

N-(6-bromo-2-oxo-2*H*-chromen-3-yl)-3-chlorobenzamide (**4g**)

The title compound was prepared from **2b** (0.24 g, 1.0 mmol) and 2-chloro benzoic acid **3g** (0.17 g, 1.1 mmol) according to general procedure, to yield an off white solid. Yield: 58%; m.p.: >200 °C; Rf = 0.49 (hexane-ethyl acetate, 3:1); IR (KBr): 3400, 3003, 1750, 1604, 1476, 1425, 1230 cm^{-1}; ^{1}H NMR (DMSO-d$_6$): δ 9.23 (s, 1H, NH), 8.22 (s, 1H, H-4), 7.98 (m, 2H, ArH), 7.67 (m, 2H, H-5 and ArH), 7.42 (m, 2H, H-7 and ArH), 6.82 (d, J = 8.5 Hz, 1H, H-8); ^{13}C NMR (DMSO-d$_6$): δ 168.6, 156.2, 154.9, 135.6, 134.2, 132.7, 132.4, 132.2, 131.8, 131.3, 121.8, 119.4, 119.1, 115.8, 112.3, 110.5. HRMS (ESI) m/z: calcd. for C$_{16}$H$_9$BrClNO$_3$ [M + H]$^+$: 377.9532, found: 377.9524.

N-(6-bromo-2-oxo-2*H*-chromen-3-yl)-2-iodobenzamide (**4h**)

The title compound was prepared from **2b** (0.24 g, 1.0 mmol) and 2-iodo benzoic acid **3h** (0.27 g, 1.1 mmol) according to general procedure, to yield an off white solid. Yield: 90%; m.p.: 135–138 °C; Rf = 0.42 (hexane-ethyl acetate, 3:1); IR (KBr): 3409, 3062, 1683, 1582, 1466, 1404, 1268 cm^{-1}; ^{1}H NMR (DMSO-d$_6$): δ 8.27 (s, 1H, H-4), 7.97 (d, J = 7.5 Hz, 1H, ArH), 7.69 (m, 2H, H-5 and ArH), 7.46 (m, 2H, H-7 and ArH), 7.21 (m, 1H, ArH), 6.83 (d, J = 8.5 Hz, 1H, H-8); ^{13}C NMR (DMSO-d$_6$): δ 168.9, 161.4, 151.5, 142.2, 141.0, 137.4, 132.9, 131.6, 130.5, 128.7, 126.3, 124.8, 121.2, 119.6, 116.8, 94.5. HRMS (ESI) m/z: calcd. for C$_{16}$H$_9$BrINO$_3$ [M + H]$^+$: 469.8888, found: 469.8321.

N-(6-bromo-2-oxo-2*H*-chromen-3-yl)-4-nitrobenzamide (**4i**)

The title compound was prepared from **2b** (0.24 g, 1.0 mmol) and 4-nitro benzoic acid **3i** (0.18 g, 1.1 mmol) according to general procedure, to yield an off white solid. Yield: 60%; m.p.: >200 °C; Rf = 0.48 (hexane-ethyl acetate, 3:1); IR (KBr): 3117, 3063, 1694, 1607, 1542, 1430, 1351, 1294 cm^{-1}; ^{1}H NMR (DMSO-d$_6$): δ 9.25 (s, 1H, NH), 8.26 (m, 3H, H-4

and ArH), 8.10 (m, 2H, ArH), 7.68 (d, J = 2.0 Hz, 1H, H-5), 7.37 (m, 1H, H-7), 6.91 (m, 1H, H-8); ^{13}C NMR (DMSO-d_6): δ 168.2, 161.6, 151.8, 150.7, 140.3, 137.6, 134.2, 130.2, 129.3, 126.8, 124.8, 122.1, 119.3, 118.2, 117.2. HRMS (ESI) m/z: calcd. for $C_{16}H_9BrN_2O_5$ [M + H]$^+$: 388.9773, found: 388.9716.

N-(6-bromo-2-oxo-2*H*-chromen-3-yl)-2-hydroxy-3,5-dinitrobenzamide (**4j**)

The title compound was prepared from **2b** (0.24 g, 1.0 mmol) and 3,5-dinitrosalicylic acid **3j** (0.25 g, 1.1 mmol) according to general procedure, to yield a yellow solid. Yield: 68%; m.p.: >200 °C; Rf = 0.43 (hexane-ethyl acetate, 3:1); IR (KBr): 3259, 3071, 1695, 1600, 1569, 1494, 1415, 1322, 1271 cm^{-1}; ^{1}H NMR (DMSO-d_6/CDCl$_3$; 1:1): δ 13.32 (s, 1H, OH), 8.64 (m, 2H, ArH), 8.24 (s, 1H, H-4), 7.63 (s, 1H, H-5), 7.47 (m, 1H, H-7), 6.84 (m, 1H, H-8); ^{13}C NMR (DMSO-d_6/CDCl$_3$; 1:1): δ 164.2, 161.2, 159.6, 149.9, 141.1, 137.1, 134.9, 131.2, 130.1, 126.3, 124.1, 123.1, 121.6, 119.2, 118.5, 117.1. HRMS (ESI) m/z: calcd. for $C_{16}H_8BrN_3O_8$ [M]$^+$: 448.9495, found: 448.8767.

N-(6-bromo-2-oxo-2*H*-chromen-3-yl)-2-methylbenzamide (**4k**)

The title compound was prepared from **2b** (0.24 g, 1.0 mmol) and toluic acid **3k** (0.14 g, 1.1 mmol) according to general procedure, to yield an off white solid. Yield: 96%; m.p.: 110–112 °C; Rf = 0.60 (hexane-ethyl acetate, 3:1); IR (KBr): 3300, 2949, 2809, 1739, 1693, 1610, 1430, 1226 cm^{-1}; ^{1}H NMR (DMSO-d_6): δ 8.31 (s, 1H, H-4), 7.77 (m, 2H, H-5, ArH), 7.45 (m, 2H, H-7 and ArH), 7.24 (m, 1H, ArH), 6.71 (m, 2H, H-8 and ArH), 2.47 (s, 3H, CH$_3$); ^{13}C NMR (DMSO-d_6): δ 169.2, 156.2, 149.5, 139.4, 132.9, 132.4, 132.2, 131.7, 131.0, 130.6, 126.3, 124.4, 122.8, 120.2, 118.9, 110.5, 21.8. HRMS (ESI) m/z: calcd. for $C_{17}H_{12}BrNO_3$ [M + H]$^+$: 358.0079, found: 358.5027.

N-(6-bromo-2-oxo-2*H*-chromen-3-yl)-2-hydroxybenzamide (**4l**)

The title compound was prepared from **2b** (0.24 g, 1.0 mmol) and 2-hydroxy benzoic acid **3l** (0.15 g, 1.1 mmol) according to general procedure, to yield a white solid. Yield: 92%; m.p.: 205–207 °C; Rf = 0.42 (hexane-ethyl acetate, 3:1); IR (KBr): 3400, 3000, 1750, 1606, 1443, 1220 cm^{-1}; ^{1}H NMR (DMSO-d_6): δ 9.54 (s,1H, OH), 8.31 (s, IH, H-4), 7.70 (m, 2H, H-5 and ArH), 7.45 (d, J = 8.5 Hz, 1H, H-7), 7.22 (m, 1H, ArH), 6.83 (d, J = 8.5 Hz, 1H, H-8), 6.71 (m, 2H, ArH); ^{13}C NMR (DMSO-d_6): δ 164.6, 160.2, 158.4, 151.2, 135.1, 134.2, 133.5, 132.5, 130.5, 128.6, 124.8, 123.2, 122.5, 121.9, 119.1, 112.2. HRMS (ESI) m/z: calcd. for $C_{16}H_{10}BrNO_4$ [M + H]$^+$: 359.9871, found: 359.9865.

5-Amino-*N*-(6-bromo-2-oxo-2*H*-chromen-3-yl)-2-hydroxybenzamide (**4m**)

The title compound was prepared from **2b** (0.24 g, 1.0 mmol) and 5-amino salicylic acid **3m** (0.16 g, 1.1 mmol) according to general procedure, to yield an off white solid. Yield: 82%; m.p.: 220 °C; Rf = 0.42 (hexane-ethyl acetate, 3:2); IR (KBr): 3410, 3003, 749, 1605, 1477, 1425, 1266, 1230 cm^{-1}; ^{1}H NMR (DMSO-d_6/CDCl$_3$; 1:2): δ 10.2 (s, 1H, OH), 8.21 (s, 1H, H-4), 7.72 (s, 1H, H-5), 7.45 (d, J = 8.0 Hz, 1H, H-7), 7.21 (m, 1H, ArH), 6.87 (d, J = 8.0 Hz, 1H, H-8), 6.76 (m, 2H, ArH), 4.54 (bs, 2H, NH$_2$); ^{13}C NMR (DMSO-d_6/CDCl$_3$; 1:2): δ 166.6, 158.8, 153.7, 150.1, 139.3, 132.2, 130.7, 130.6, 130.0, 129.7, 124.8, 121.4, 120.8, 116.7, 116.5, 110.3. HRMS (ESI) m/z: calcd. for $C_{16}H_{11}BrN_2O_4$ [M + H]$^+$: 374.9980, found: 374.4202.

N-(6-bromo-2-oxo-2*H*-chromen-3-yl)-2-hydroxy-3,5-diiodobenzamide (**4n**)

The title compound was prepared from **2b** (0.24 g, 1.0 mmol) and 3,5-diiodo salicylic acid **3n** (0.42 g, 1.1 mmol) according to general procedure, to yield a white solid. Yield: 70%; m.p.: 195 °C; Rf = 0.38 (hexane-ethyl acetate, 3:1); IR (KBr): 3407, 3003, 1749, 1667, 1476, 1425, 1229 cm^{-1}; ^{1}H NMR (DMSO-d_6/CDCl$_3$; 1:1): δ 10.15 (s, 1H, OH), 8.22 (s, 1H, H-4), 8.13 (s, 1H, ArH), 7.99 (s, 1H, ArH), 7.72 (s, 1H, H-5), 7.45 (d, J = 8.5 Hz, 1H, H-7), 6.84 (d, J = 8.5 Hz, 1H, H-8); ^{13}C NMR (DMSO-d_6/CDCl$_3$; 1:1): δ 170.4, 168.5, 162.0, 156.1, 149.4, 138.7, 132.8, 132.5, 132.3, 122.0, 118.9, 118.5, 110.6, 88.8, 79.5. HRMS (ESI) m/z: calcd. for $C_{16}H_8BrI_2NO_4$ [M + H]$^+$: 611.7804, found: 611.7716.

N-(6-bromo-2-oxo-2*H*-chromen-3-yl)-3,4,5-trihydroxybenzamide (**4o**)

The title compound was prepared from **2p** (0.24 g, 1.0 mmol) and gallic acid **3o** (0.18 g, 1.1 mmol) according to general procedure, to yield an off white solid. Yield: 92%; m.p.: 155 °C; Rf = 0.41 (hexane-ethyl acetate, 3:2); IR (KBr): 3322, 3000, 1738, 1609, 1496, 1429, 1365, 1267 cm^{-1}; ^{1}H NMR (DMSO-d$_6$): δ 9.74 (s, 1H, OH), 9.01 (s 1H, OH), 8.14 (s, 1H, H-4), 7.75 (s, 1H, H-5), 7.45 (m, 1H, H-7), 7.38 (m, 2H, ArH), 6.87 (m, 1H, H-8); ^{13}C NMR (DMSO-d$_6$): δ 165.8, 157.0, 152.8, 142.6, 141.4, 140.4, 134.3, 132.7, 130.2, 129.0, 125.0, 121.5, 118.5, 116.2, 117.0, 109.9. HRMS (ESI) m/z: calcd. for C$_{16}$H$_{10}$BrNO$_6$ [M + H]$^{+}$: 391.9769, found: 391.9221.

N-(6-bromo-2-oxo-2*H*-chromen-3-yl)pyrrolidine-2-carboxamide (**4p**)

The title compound was prepared from **2b** (0.24 g, 1.0 mmol) and L-proline **3p** (0.12 g, 1.1 mmol) according to general procedure, to yield a light brown solid. Yield: 66%; m.p.: 224 °C; Rf = 0.52 (hexane-ethyl acetate, 3:1); IR (KBr): 3400, 3006, 2951, 2725, 2610, 1750, 1604, 1476, 1316, 1266 cm^{-1}; ^{1}H NMR (CDCl$_3$): δ 8.50 (s, 1H, NH), 8.13 (s, 1H, H-4), 7.68 (s, 1H, H-5), 7.43 (d, J = 8.5 Hz, 1H, H-7), 6.86 (d, J = 8.5 Hz, 1H, H-7), 4.07 (m, 1H, NCH), 3.59 (m, 2H, NCH$_2$), 2.41 (m, 2H, CH$_2$), 1.82 (m, 2H, CH$_2$); ^{13}C NMR (DMSO-d$_6$/CDCl$_3$; 1:2): δ 168.2, 160.1, 149.4, 137.1, 132.6, 130.2, 125.6, 121.2, 119.4, 116.8, 61.4, 45.4, 32.1, 24.2. HRMS (ESI) m/z: calcd. for C$_{14}$H$_{13}$BrN$_2$O$_3$ [M + H]$^{+}$: 337.0188, found: 337.0194.

3.3. Biology

3.3.1. Evaluation of Antiquorum Sensing Activity of Compounds for Biofilm Inhibition

The antiquorum sensing activity of the compound series was evaluated by biosensor bioassay with the *Chromobacterium violaceum* CV026 strain using the agar well diffusion method [33]. A bacterial lawn was developed on agar plates by using freshly prepared *C. violaceum* culture in Luria Bertani (LB) medium. The wells were inoculated with 100 μL of stock solution of 2 mg/mL of compounds. These plates were incubated at 27 °C for 48 h. DMSO was used as negative control. The antiquorum sensing activity was determined in terms of the zone of inhibition (measured in mm) developed around the wells. Compounds showing positive results on agar plates were subjected to biofilm inhibition analysis.

3.3.2. Biofilm Formation

Biofilm of Gram-negative *Pseudomonas aeruginosa* PAO1 was formed on glass wool in Petri plates (25 mm) filled with freshly prepared 10 mL culture in nutrient broth. These plates were incubated under static conditions at 37 °C for 48 h. After incubation, biofilm grown on glass wool was observed and analyzed.

3.3.3. Biofilm Inhibition Analysis

Biofilm inhibition and degradation tests were carried out in 96-well microtiter plates using the crystal violet (CV) staining method as described by Shukla et al. [33]. A 100 μL volume of freshly prepared *P. aeruginosa* suspension was taken in a 96-well plate, and 100 μL of 0.2 mg/mL stock of the test compound was added to each well and incubated for 48 h at 37 °C. After incubation, planktonic cells were removed by removing excess media and washing the wells with distilled water. A 200 μL volume of 0.4% CV dye was further added to each well and incubated for 20 min to stain cells of the attached biofilm. This was followed by washing of wells with distilled water to remove excess dye, and plates were dried. For analysis, the biofilm was resolubilized in DMSO, and a reading was taken at 620 nm with an ELISA reader. The percentage biofilm inhibited by the test compounds was calculated by the following formula

$$\% \text{ of Biofilm inhibition} = \frac{\text{OD}_{620nm}\text{in control} - \text{OD}_{620nm}\text{in treatment}}{\text{OD}_{620nm}\text{in control}} \times 100$$

3.4. Molecular Docking

All the synthesized compounds were docked using Auto-Dock Tools (ADT version 1.5.6, The Scripps Research Institute, La Jolla, CA, USA) and AutoDock version 4.0. The high-resolution crystal structure of *P. aeruginosa* the LasR ligand-binding domain bound to its autoinducer with PDB ID: 2UV0 was retrieved from the Protein Data Bank (www.rcsb.org (8 December 2021)). A self-predicted active site having grid X-Y-Z coordinates: 23.900, 15.715, 80.896 Å and spacing 1.000 Å was taken for the calculation. This active pocket consists of 17 amino acids. Initially, the 3D structures of ligands were drawn using ACD/ChemSketch and saved in MDL Molfiles [V2000] format. The MDL Molfiles were further converted into .pdb format using the Open Babel GUI. Then, the environment was created for protein preparation in ADT consecutively polar hydrogens, and Kollman charges were added. The formats of both the protein and ligand files were changed to pdbqt format as only this particular format is operational in ADT GUI. The docking tool operated on the Lamarckian genetic algorithm and yielded various docked poses, among which the top ten runs were considered on the basis of the scoring function. Root mean square deviation (RMSD) values differing by less than 0.5 Å were taken into account to generate docked ligands of our interest. The ligand–protein docked conformations were studied and evaluated on the basis of various parameters such as binding energy, hydrogen bonding and hydrophobic interactions existing between the binding ligand and receptor protein. For visualization of various docking poses, coordinates and interactions, we used the software Chimera 1.8.1 (University of California, San Francisco, CA, USA).

4. Conclusions

In conclusion, we synthesized a series of sixteen amidocoumarins as potential biofilm inhibitors. Compounds **4f**, **4l** and **4o** inhibited the biofilm formation in antibiotic-resistant *P. aeruginosa* PAO1 in the range of 80 to 86% at 100 µg/mL compound. This study also provides preliminary SARs around the 3-amidocoumarin motif. The presence of the bromo group at the C-6 position of the coumarin ring was favorable for bioactivity. The electron-donating groups at amido moiety enhance the antibiofilm activity. while electron-withdrawing groups result in reduced antibiofilm properties of the compounds. The SAR data could further help in the development of newer 3-amidocoumarin-based potential biofilm inhibitors. The in silico study revealed that coumarins compounds occupied the active site of the LasR receptor. The binding energy from molecular docking ranged from −9.44 to −11.69 kcal/mol. The best results of the docking studies were obtained with compounds **4h**, **4l** and **4o**. The results showed that this study might hold promise in the design and development of safe and effective inhibitors of biofilm and QS as an alternative therapy.

Author Contributions: Conceptualization, V.S. and D.K.; Methodology, R.K.S., V.S. and V.R.; Formal analysis, R.K.S., V.S. and D.K.; Investigation, R.K.S., V.S. and D.K.; Writing—Original Draft Preparation, R.K.S. and D.K.; Writing—Review and Editing, V.S., V.R. and D.K.; Funding Acquisition, D.K. All authors have read and agreed to the published version of the manuscript.

Institutional Review Board Statement: Not applicable.

Informed Consent Statement: Not applicable.

Data Availability Statement: All data are included in the article and/or Supplementary Materials.

Conflicts of Interest: The authors declare no competing interests.

References

1. Vestby, L.K.; Grønseth, T.; Simm, R.; Nesse, L.L. Bacterial biofilm and its role in the pathogenesis of disease. *Antibiotics* **2020**, *9*, 59. [CrossRef] [PubMed]
2. Jamal, M.; Ahmad, W.; Andleeb, S.; Jalil, F.; Imran, M.; Nawaz, M.A.; Hussain, T.; Ali, M.; Rafiq, M.; Kamil, M.A. Bacterial biofilm and associated infections. *J. Chin. Med. Assoc.* **2018**, *81*, 7–11. [CrossRef] [PubMed]
3. Roy, R.; Tiwari, M.; Donelli, G.; Tiwari, V. Strategies for combating bacterial biofilms: A focus on anti-biofilm agents and their mechanisms of action. *Virulence* **2018**, *9*, 522–554. [CrossRef] [PubMed]
4. Antimicrobial Resistance Collaborators. Global burden of bacterial antimicrobial resistance in 2019: A systematic analysis. *Lancet* **2022**, *399*, 629–655. [CrossRef]
5. Hall, C.W.; Mah, T.-F. Molecular mechanisms of biofilm-based antibiotic resistance and tolerance in pathogenic bacteria. *FEMS Microbiol. Rev.* **2017**, *41*, 276–301. [CrossRef]
6. Rabin, N.; Zheng, Y.; Opoku-Temeng, C.; Du, Y.; Bonsu, E.; Sintim, H.O. Biofilm formation mechanisms and targets for developing antibiofilm agents. *Future Med. Chem.* **2015**, *7*, 493–512. [CrossRef]
7. Koo, H.; Allan, R.N.; Howlin, R.P.; Stoodley, P.; Stoodley, L.H. Targeting microbial biofilms: Current and prospective therapeutic strategies. *Nat. Rev. Microbiol.* **2017**, *15*, 740–755. [CrossRef]
8. Preda, V.G.; Săndulescu, O. Communication is the key: Biofilms, quorum sensing, formation and prevention. *Discoveries* **2019**, *7*, e100. [CrossRef]
9. Sionov, R.V.; Steinberg, D. Targeting the holy triangle of quorum sensing, biofilm formation, and antibiotic resistance in pathogenic bacteria. *Microorganisms* **2022**, *10*, 1239. [CrossRef]
10. Whiteley, M.; Diggle, S.; Greenberg, E. Progress in and promise of bacterial quorum sensing research. *Nature* **2017**, *551*, 313–320. [CrossRef]
11. Miller, M.B.; Bassler, B.L. Quorum sensing in bacteria. *Annu. Rev. Microbiol.* **2001**, *55*, 165–199. [CrossRef]
12. Rutherford, S.T.; Bassler, B.L. Bacterial quorum sensing: Its role in virulence and possibilities for its control. *Cold Spring Harb. Perspect. Med.* **2012**, *2*, a012427. [CrossRef]
13. Ramanathan, S.; Sivasubramanian, S.; Pandurangan, P.; Mani, G.; Madhu, D.; Lin, X. Bacterial biofilm inhibition: A focused review on recent therapeutic strategies for combating the biofilm mediated infections. *Front. Microbiol.* **2021**, *12*, 676458. [CrossRef]
14. Nadar, S.; Khan, T.; Patching, S.G.; Omri, A. Development of antibiofilm therapeutics strategies to overcome antimicrobial drug resistance. *Microorganisms* **2022**, *10*, 303. [CrossRef]
15. Manefield, M.; de Nys, R.; Kumar, N.; Read, R.; Givskov, M.; Steinberg, P.; Kjelleberg, S.A. Evidence that halogenated furanones from *Delisea pulchra* inhibit acylated homoserine lactone (AHL)-mediated gene expression by displacing the AHL signal from its receptor protein. *Microbiology* **1999**, *145*, 283–291. [CrossRef]
16. Park, J.S.; Ryu, E.-J.; Li, L.; Choi, B.-K.; Kim, B.M. New bicyclic brominated furanones as potent autoinducer-2 quorum-sensing inhibitors against bacterial biofilm formation. *Eur. J. Med. Chem.* **2017**, *137*, 76–87. [CrossRef]
17. Yang, S.; Abdel-Razek, O.A.; Cheng, F.; Bandyopadhyay, D.; Shetye, G.S.; Wang, G.; Luk, Y.-Y. Bicyclic brominated furanones: A new class of quorum sensing modulators that inhibit bacterial biofilm formation. *Bioorg. Med. Chem.* **2014**, *22*, 1313–1317. [CrossRef]
18. Almohaywi, B.; Yu, T.T.; Iskander, G.; Chan, D.S.H.; Ho, K.K.K.; Rice, S.; Black, D.S.; Griffith, R.; Kumar, N. Dihydropyrrolones as bacterial quorum sensing inhibitors. *Bioorg. Med. Chem. Lett.* **2019**, *29*, 1054–1059. [CrossRef]
19. Liu, Z.; Zhang, P.; Qin, Y.; Zhang, N.; Teng, Y.; Venter, H.; Ma, S. Design and synthesis of aryl-substituted pyrrolidone derivatives as quorum sensing inhibitors. *Bioorg. Chem.* **2020**, *105*, 104376. [CrossRef]
20. Nizalapur, S.; Kimyon, O.; Yee, E.; Bhadbhade, M.M.; Manefield, M.; Willcox, M.; Black, D.S.C.; Kumar, N. Synthesis and biological evaluation of novel acyclic and cyclic glyoxamide based derivatives as bacterial quorum sensing and biofilm inhibitors. *Org. Biomol. Chem.* **2017**, *15*, 5743–5755. [CrossRef]
21. Singh, L.R.; Tripathi, V.C.; Raj, S.; Kumar, A.; Gupta, S.; Horam, S.; Upadhyay, A.; Kushwaha, P.; Arockiaraj, J.; Sashidhara, K.V.; et al. In-house chemical library repurposing: A case example for *Pseudomonas aeruginosa* antibiofilm activity and quorum sensing inhibition. *Drug Dev. Res.* **2018**, *9*, 383–390. [CrossRef] [PubMed]
22. Stowe, S.D.; Richards, J.J.; Tucker, A.T.; Thompson, R.; Melander, C.; Cavanagh, J. Anti-biofilm compounds derived from marine sponges. *Mar. Drugs* **2011**, *9*, 2010–2035. [CrossRef] [PubMed]

23. Herrera, K.M.S.; da Silva, F.K.; de Lima, W.G.; de Barbosa, S.C.; Gonçalves, A.M.M.N.; Viana, G.H.R.; Soares, A.C.; Ferreira, J.M.S. Antibacterial and antibiofilm activities of synthetic analogs of 3-alkylpyridine marine alkaloids. *Med. Chem. Res.* **2020**, *29*, 1084–1089. [CrossRef]

24. El-Messery, S.M.; Habib, E.E.; Al-Rashood, S.T.A.; Hassan, G.S. Synthesis, antimicrobial, anti-biofilm evaluation, and molecular modelling study of new chalcone linked amines derivatives. *J. Enzyme Inhib. Med. Chem.* **2018**, *33*, 818–832. [CrossRef]

25. Mairink, S.Z.; Barbosa, L.C.A.; Boukouvalas, J.; Pedroso, S.H.S.P.; Santos, S.G.; Magalhães, P.P.; Farias, L.M. Synthesis and evaluation of cadiolide analogues as inhibitors of bacterial biofilm formation. *Med. Chem. Res.* **2018**, *27*, 2426–2436. [CrossRef]

26. Lal, J.; Kaul, G.; Akhir, A.; Ansari, S.B.; Chopra, S.; Reddy, D.N. Bio-evaluation of fluoro and trifluoromethyl-substituted salicylanilides against multidrug-resistant *S. aureus*. *Med. Chem. Res.* **2021**, *30*, 2301–2315. [CrossRef]

27. Reen, F.J.; Gutiérrez-Barranquero, J.; Parages, M.L.; O'Gara, F. Coumarin: A novel player in microbial quorum sensing and biofilm formation inhibition. *Appl. Microbiol. Biotechnol.* **2018**, *102*, 2063–2073. [CrossRef]

28. Lee, J.H.; Kim, Y.G.; Cho, H.S.; Ryu, S.Y.; Cho, M.H.; Lee, J. Coumarins reduce biofilm formation and the virulence of *Escherichia coli* O157:H7. *Phytomedicine* **2014**, *21*, 1037–1042. [CrossRef]

29. D'Almeida, R.E.; Molina, R.D.I.; Viola, C.M.; Luciardi, M.C.; Peñalver, C.N.; Bardón, A.; Arena, M.E. Comparison of seven structurally related coumarins on the inhibition of quorum sensing of *Pseudomonas aeruginosa* and *Chromobacterium violaceum*. *Bioorg. Chem.* **2017**, *73*, 37–42. [CrossRef]

30. Ojima, Y.; Nunogami, S.; Taya, M. Antibiofilm effect of warfarin on biofilm formation of *Escherichia coli* promoted by antimicrobial treatment. *J. Glob. Antimicrob. Resist.* **2016**, *7*, 102–105. [CrossRef]

31. Qais, F.A.; Khan, M.S.; Ahmad, I.; Husain, F.M.; Khan, R.A.; Hassan, I.; Shahzad, S.A.; AlHarbi, W. Coumarin exhibits broad-spectrum antibiofilm and antiquorum sensing activity against Gram-negative bacteria: In vitro and in silico investigation. *ACS Omega* **2021**, *6*, 18823–18835. [CrossRef]

32. Sharma, R.K.; Singh, V.; Tiwari, N.; Butcher, R.J.; Katiyar, D. Synthesis, antimicrobial and chitinase inhibitory activities of 3-amidocoumarins. *Bioorg. Chem.* **2020**, *98*, 103700. [CrossRef]

33. Shukla, M.; Singh, V.; Habeeballah, H.; Alkhanani, M.F.; Lata, M.; Hussain, Y.; Mukherjee, M.; Pasupuleti, M.; Meena, A.; Mishra, B.N.; et al. Quorum quenching guided inhibition of mixed bacterial biofilms and virulence properties by protein derived from leaves of *Carissa carandas*. *Front. Cell. Infect. Microbiol.* **2022**, *12*, 836819. [CrossRef]

34. Sharma, R.K.; Priyanka; Katiyar, D. L-proline catalyzed condensation of salicylaldehydes with ethyl nitroacetate: An efficient access to 3-nitrocoumarins. *Monatsh. Chem.* **2016**, *147*, 2157–2161. [CrossRef]

35. Hentzer, M.; Wu, H.; Andersen, J.B.; Riedel, K.; Rasmussen, T.B.; Bagge, N.; Kumar, N.; Schembri, M.A.; Song, Z.; Kristoffersen, P.; et al. Attenuation of *Pseudomonas aeruginosa* virulence by quorum sensing inhibitors. *EMBO J.* **2003**, *22*, 3803–3815. [CrossRef]

36. Bottomley, M.J.; Muraglia, E.; Bazzo, R.; Carfi, A. Molecular insights into quorum sensing in the human pathogen *Pseudomonas aeruginosa* from the structure of the virulence regulator LasR bound to its autoinducer. *J. Biol. Chem.* **2007**, *282*, 13592–13600. [CrossRef]

37. Gavrilova, N.A.; Semichenko, E.S.; Korotchenko, O.S.; Suboch, G.A. Cyclocondensation of ethyl nitroacetate with 2-hydroxybenzaldehydes. *Russ. J. Org. Chem.* **2008**, *44*, 624–625. [CrossRef]

38. Das, D.K.; Sarkar, S.; Khan, M.; Belal, M.; Khan, A.T. A mild and efficient method for large scale synthesis of 3-aminocoumarins and its further application for the preparation of 4-bromo-3-aminocoumarins. *Tetrahedron Lett.* **2014**, *55*, 4869–4874. [CrossRef]